

M³-AUDIODEC: MULTI-CHANNEL MULTI-SPEAKER MULTI-SPATIAL AUDIO CODEC

Anton Ratnarajah¹, Shi-Xiong Zhang², Dong Yu²

¹ University of Maryland, College Park, MD, USA ² Tencent AI Lab, Bellevue, WA, USA

ABSTRACT

We introduce M³-AUDIODEC, an innovative neural spatial audio codec designed for efficient compression of multi-channel (binaural) speech in both single and multi-speaker scenarios, while retaining the spatial location information of each speaker. This model boasts versatility, allowing configuration and training tailored to a predetermined set of multi-channel, multi-speaker, and multi-spatial overlapping speech conditions. Key contributions are as follows: 1) Previous neural codecs are extended from single to multi-channel audios. 2) The ability of our proposed model to compress and decode for overlapping speech. 3) A groundbreaking architecture that compresses speech content and spatial cues separately, ensuring the preservation of each speaker’s spatial context after decoding. 4) M³-AUDIODEC’s proficiency in reducing the bandwidth for compressing two-channel speech by 48% when compared to individual binaural channel compression. Impressively, at a 12.6 kbps operation, it outperforms Opus at 24 kbps and AUDIODEC at 24 kbps by 37% and 52%, respectively. In our assessment, we employed speech enhancement and room acoustic metrics to ascertain the accuracy of clean speech and spatial cue estimates from M³-AUDIODEC. Audio demonstrations and source code are available online¹.

Index Terms— binaural audio codec, spatial audio codec

1. INTRODUCTION

Neural audio codecs (NACs) compress audio signals to minimize data storage and transmission. Present-day NACs can be grouped into hybrid techniques, which fuse conventional audio coding with neural speech synthesis [1–3], and end-to-end approaches [4–7]. The latter offers notable enhancements in audio quality and adapts to varying audio content. However, most existing NACs target single-channel audio and single-speaker optimization [7]. Recognizing these gaps, our work introduces M³-AUDIODEC, a spatial audio codec tailored for efficient compression in multi-channel and multi-speaker contexts.

A key difference between single-channel and multi-channel audio is the latter’s encapsulation of spatial localization alongside pure speech content ($S[t]$) [8]. This spatial

context manifests in various acoustic facets such as early reflections, late reverberations, interaural time difference (ITD) and interaural level difference (ILD) between microphones. Mathematically, these aspects can be represented through the impulse response (IR) function, allowing the breakdown of speech content and multi-channel effects as:

$$B[t] = S[t] \otimes IR[t]. \quad (1)$$

For overlapped multi-channel speech ($OB[t]$) with a fixed number of multiple speakers (M_S) in multiple different spatial locations, we can decompose their clean speech content $S_i[t]$ and their multi-channel IRs $IR_i[t]$ separately as follows:

$$OB[t] = \sum_{i=1}^{M_S} (S_i[t] \otimes IR_i[t]). \quad (2)$$

Main Contribution: We present a pioneering NAC architecture optimized for multi-channel multi-speaker overlapped speech, crucially retaining each speaker’s spatial details. This architecture is illustrated in Fig.1. In contrast to the existing AUDIODEC model [7], our key contributions are: 1) expanding codec capabilities to multi-channel audio; 2) efficient overlapping speech compression; 3) separate compression of speech content and spatial cues; 4) achieving a high compression rate for multi-channel audio. Our model, operating at 12.6 kbps, can reconstruct a 48 kHz binaural speech signal with two spatially distinct speakers, significantly surpassing AUDIODEC and outperforming Opus [9] and Encdec [5]. Supplementary materials, including speech samples, spectrograms, and source code, are provided for future research¹.

2. RELATED WORLD

Traditional audio codecs: Linear predictive coding-based audio codecs [10,11] and model-based audio codecs [12] have been proposed in the past for speech coding, but their quality is limited. Among the traditional methods, Opus [9] and EVS [13] are state-of-the-art traditional audio codec architecture, and they can support different bitrates and sampling rates at high coding efficiency in real-time.

Neural audio codecs: End-to-end data-driven architectures are proposed to code mono and stereo audio with impressive performance [4–6]. The Encdec [5] can compress stereo audio by separately processing the left and right channels. This approach results in poor compression of stereo audio because the same speech content in both channels is coded twice. Our M³-AUDIODEC (MAD) can significantly reduce

¹<https://anton-geran.github.io/MAD/>

the bandwidth by coding the speech content only once. Also, our network is efficiently designed to compress overlapped speech while preserving individual speakers’ speech content and spatial acoustic features.

Speech dereverberation and RIR Estimation: Recently, NAC-based architectures have been proposed for audio-visual speech enhancement [14]. Similarly, in our work, we decode clean speech from multi-channel speech. Generative architectures are recently been proposed to estimate IR for the given spatial information [15, 16]. Encoder-decoder architectures have shown promising results in estimating IR from the reverberant speech signal [17, 18]. We propose NAC to estimate IR of one-second duration from multi-channel speech.

3. M³-AUDIODEC

We propose NAC to compress multi-channel (M_C) speech recording $B(x)$ with a sampling rate of 48 kHz. Similar to typical NAC [4, 7], our model consists of an encoder, projector, quantizer and decoder modules. We propose simple and complex decoder architecture for single-speaker and multi-speaker (M_S) scenarios, respectively. Our proposed encoder architecture is the same for single-speaker and multi-speaker cases. We adapt the projector and quantizer from the AUDIODEC [7].

3.1. Encoder Architecture

We pass the multi-channel speech to a common encoder consisting of a 1D Convolutional layer (CONV) with a kernel size (K) of 3, stride (S) 1 and the same number of input channels (IC = M_C) and output channels (OC). We pass the common encoder network output to the speech encoder and multi-channel IR encoder. The speech encoder follows the same architecture as AUDIODEC [7] and SoundStream [4]. Speech Encoder has a CONV (K = 7, S = 1, IC = M_C , OC = $8 * M_C$) followed by convolution blocks C_{B1} . Each C_{B1} has three residual units (RU) with dilated CONV (dilation rates are 1, 3 and 9) followed by a CONV (K = $2 * S$, S = S, IC = IC, OC = $2 * IC$). We have 5 C_{B1} s with S = (2, 2, 3, 5, 5). Therefore, we downsample the speech content by a factor of 300. Our IR encoder is motivated by the IR estimator network [17]. The IR encoder has three CONV blocks C_{B2} . Each C_{B2} has CONV followed by batch normalization (BN) and leaky ReLU. First C_{B2} does not have BN. The three C_{B2} has OC = ($M_C * 64$, $M_C * 128$, $M_C * 256$), K = (96001, 41, 41), S = (1500, 2, 2) and padding (P) = (48000, 20, 20). We significantly down-sample IR content by a factor of 6000. All the CONVs are causal to make the network work in real time. The speech encoder and IR encoder output is projected to multi-dimensional space separately and quantized into codes using projector and quantizer modules proposed in AUDIODEC.

3.2. Decoder Architecture

We propose two different architectures for the single-speaker and multi-speaker scenarios as follows:

Single speaker: We propose a speech decoder architecture to decode the clean speech and an IR decoder to decode multi-channel IR. We reconstruct the multi-channel speech from estimated clean speech and IR using Eq. 1. Both speech and IR decoders adapt the SoundStream decoder. Before inputting to decoder modules, we pass the code to CONV (IC = $M_C * 32$, OC = 512, K = 7, S = 1). The speech decoder has 5 CONV blocks C_{B3} with S = (5, 5, 3, 2, 2) followed by CONV with OC = 1, K = 7 and S = 1. Each C_{B3} has transposed convolutional layers (IC = IC, OC = $0.5 * IC$, K = $2 * S$, S) followed by three RU similar to the encoder. IR decoder has a similar network as the speech decoder except for the number of C_{B3} . IR decoder has 6 C_{B3} s with S = (5, 5, 5, 4, 3, 2) and the final CONV has M_C output channels. We reconstruct clean speech of two-second duration and one-second multi-channel IR with a sampling rate of 48kHz.

Multi speakers: For the multi-speaker scenario, we replicate the speech decoder in the single-speaker scenario M_S times to decode the clean speech of M_S speakers. We perform speech separation in the decoder to force the network to preserve the speech content of individual speakers in the code. Instead of directly passing the output C of the CONV layer, we learn the representation of each speaker S_i by learning mask vector $M_i \in [0, 1]$. Similar to Conv-TasNet [19], the S_i is calculated by performing element-wise multiplication of C and M_i . We pass S_i to the speech decoder modules to estimate the clean speech of each speaker. We use the same IR decoder as the single speaker network while we increase the number of channels of each layer by M_S times. Fig. 1 shows our model for two-speaker binaural speech ($M_S = M_C = 2$).

3.3. Training Objective

We adapt the training paradigm proposed in AUDIODEC. We train the end-to-end network with the metric loss for 200k iterations. Then we replace our speech decoders with HiFi-GAN [20] vocoders and train with the metric and adversarial loss for 500k iterations using HiFi-GAN-based multi-period and multi-scale discriminators [7]. For the multi-speaker scenario, we continue to train our end-to-end network with adversarial and metric loss after 200k iterations for an additional 160k iterations. Let $B(x)$ and $\hat{B}(x)$ denote the input and reconstructed multi-channel speech. We denote the ground truth (GT) and reconstructed clean speech of speaker i using $S_i(x)$ and $\hat{S}_i(x)$ respectively. $IR_i(x)$ and $\hat{IR}_i(x)$ represent their corresponding GT and reconstructed multi-channel IRs.

Metric Loss: We use the mel spectral loss (Eq. 3) and spectrogram loss as our metric loss for clean and multi-channel speech. In Eq. 3, MEL denotes the extraction of the mel spectrogram. \mathbb{E} denotes the expectation, and L1-norm and L2-norm are denoted by $\|\cdot\|_1$ and $\|\cdot\|_2$ respectively.

$$\mathcal{L}_{MEL}(x, \hat{x}) = \mathbb{E}[\|MEL(x) - MEL(\hat{x})\|_1]. \quad (3)$$

For spectrogram loss, we calculate the mean square difference of the log magnitude of the GT speech spectrogram

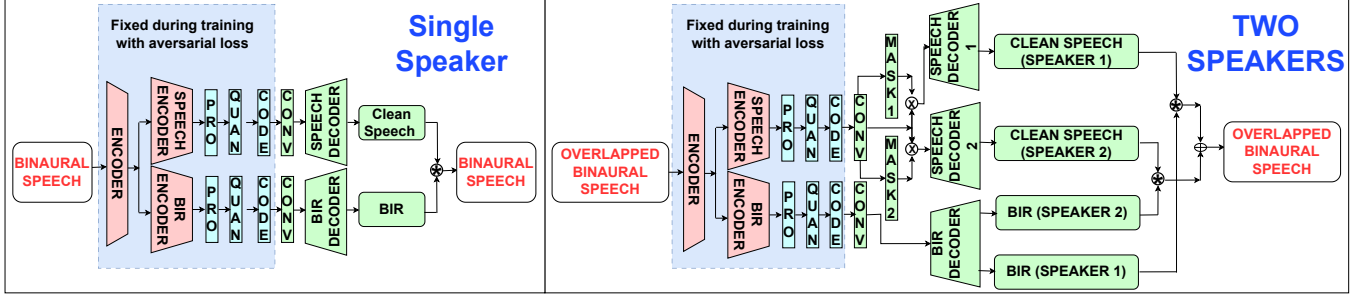


Fig. 1. Our proposed neural audio codec configured for single-speaker and two-speaker two-spatial overlapped binaural speech. In § 3, we describe the details of our architecture and training paradigm. We train end-to-end networks with metric loss (Eq. 6) for 200K iterations. Then, we freeze the blocks shown in blue and train the rest of the network with the metric and adversarial loss (Eq. 8) for an additional 500k iterations and 160k iterations for single-speaker and two-speaker cases, respectively.

($M_{spec}(x)$) and estimated speech spectrogram ($M_{spec}(\hat{x})$) (Eq. 4).

$$\mathcal{L}_{MAG}(x, \hat{x}) = \mathbb{E}[\|M_{spec}(x) - M_{spec}(\hat{x})\|_2^2]. \quad (4)$$

We calculated time-domain mean square error (MSE) between GT and estimated multi-channel IRs (Eq. 5) as our metric loss for estimated multi-channel IRs as follows:

$$\mathcal{L}_{IR}(b, \hat{b}) = \mathbb{E}[\|b - \hat{b}\|_2^2]. \quad (5)$$

Our total metric loss is defined as follows:

$$\begin{aligned} \mathcal{L}_{MET}(x) = & (\mathcal{L}_{MEL}(B(x), \hat{B}(x)) + \mathcal{L}_{MAG}(B(x), \hat{B}(x))) \\ & + \sum_{i=1}^{M_S} (\mathcal{L}_{MEL}(S_i(x), \hat{S}_i(x)) + \mathcal{L}_{MAG}(S_i(x), \hat{S}_i(x))) \\ & + \mathcal{L}_{IR}(IR_i(x), \hat{IR}_i(x))), \quad (6) \end{aligned}$$

where M_S is the total number of speakers in the speech.

Adversarial Loss: We train two HiFi-GAN discriminators for multi-channel and clean speech by optimizing the following objective function:

$$\begin{aligned} \mathcal{L}_D(x) = & \mathbb{E}[\max(0, 1 - D_B(B(x))) + \max(0, 1 + D_B(\hat{B}(x))) \\ & + \sum_{i=1}^{M_S} (\max(0, 1 - D_S(S_i(x))) + \max(0, 1 + D_S(\hat{S}_i(x))))], \quad (7) \end{aligned}$$

where D_B and D_S are the discriminators of multi-channel speech and clean speech respectively. We train our M³-AUDIODEC (MAD) with the following adversarial loss.

$$\mathcal{L}_{ADV} = \mathbb{E}[\max(0, 1 - D_B(\hat{B}(x))) + \sum_{i=1}^{M_S} \max(0, 1 - D_S(\hat{S}_i(x)))]. \quad (8)$$

In addition to the $\mathcal{L}_{MET}(x)$ and $\mathcal{L}_{ADV}(x)$, we train our network with \mathcal{L}_{VQ} [21] applied to the VQ codebook. Our overall generator loss $\mathcal{L}_{GEN}(x)$ is as follows:

$$\mathcal{L}_{GEN}(x) = \mathcal{L}_{MET}(x) + \lambda_{ADV}\mathcal{L}_{ADV} + \lambda_{VQ}\mathcal{L}_{VQ}, \quad (9)$$

where λ_{ADV} and λ_{VQ} are the weights.

4. EXPERIMENTS

Dataset: We generate binaural speech datasets ($M_C = 2$) for single-speaker and two-speaker ($M_S = 2$) cases using clean

Table 1. The baselines used for our comparison. We can see that our approach severely compresses the binaural speech. Our approach can reduce the bandwidth of AUDIODEC by up to 47.5% for binaural speech.

| Method | Compression | Bandwidth | Sampling Rate |
|--------------------|--------------|------------------|---------------|
| Opus-12 [9] | - | 12 kbps | 48 kHz |
| Opus-24 [9] | - | 24 kbps | 48 kHz |
| HiFi-Codec-320 [6] | 320x | - | 24 kHz |
| HiFi-Codec-240 [6] | 240x | - | 24 kHz |
| Encodec-12 [5] | 256x | 12 kbps | 48 kHz |
| Encodec-48 [5] | 64x | 48 kbps | 48 kHz |
| AUDIODEC [7] | 300x | 24 kbps | 48 kHz |
| MAD (Ours) | 3150x | 12.6 kbps | 48 kHz |

Table 2. Interaural time difference error (E_{ITD}) and interaural level difference errors (E_{ILD_L} , E_{ILD_R}) of final reconstructed binaural speech from the baselines (Table 1) and different variations of our model (§ 4). We also report the STOI of the intermediate estimated clean speech from our approach. We compare our single and two-speaker models (Fig. 1).

| Speakers | Method | $E_{ITD} \downarrow$ | $E_{ILD_L} \downarrow$ | $E_{ILD_R} \downarrow$ | STOI \uparrow | |
|------------|----------------|----------------------|------------------------|------------------------|-----------------|---|
| Single | Opus-12 | 30.7 ms | 1.28 | 1.28 | - | |
| | Opus-24 | 25.4 ms | 1.04 | 1.07 | - | |
| | HiFi-Codec-320 | 36.0 ms | 1.21 | 1.24 | - | |
| | HiFi-Codec-240 | 37.8 ms | 1.07 | 1.08 | - | |
| | Encodec-12 | 33.5 ms | 0.88 | 0.91 | - | |
| | Encodec-48 | 34.0 ms | 0.56 | 0.57 | - | |
| | AUDIODEC | 33.7 ms | 0.87 | 0.88 | - | |
| Single | MAD-V1 | 29.0 ms | 1.20 | 1.36 | 0.71 | |
| | MAD-V2 | 20.7 ms | 1.33 | 1.41 | 0.71 | |
| | MAD | 16.0 ms | 0.75 | 0.72 | 0.84 | |
| | Two | Opus-12 | 27.3 ms | 1.01 | 1.00 | - |
| | Two | Opus-24 | 31.2 ms | 0.71 | 0.79 | - |
| Two | Encodec-12 | 33.5 ms | 0.83 | 0.81 | - | |
| Two | Encodec-48 | 36.4 ms | 0.50 | 0.50 | - | |
| Two | MAD | 21.9 ms | 0.82 | 0.77 | 0.72 | |

speech from the Valentine dataset [22, 23] and simulated binaural IRs (BIRs) from pygsound [24]. We simulated 50k BIRs using pygsound and randomly convolved with clean speech corpora using Eq. 1 and Eq. 2 for single speaker and two speakers scenarios, respectively. We split the simulated

Table 3. BIR estimation error of our approach for single-speaker and two-speaker scenarios. Training binaural speech with spectrogram loss indirectly improves the BIR estimation significantly. BIR estimation of our network for a two-speaker scenario is comparable to a single-speaker scenario with a simple speech decoder (MAD-V1). We report the average error of two speakers for the two-speaker case.

| Speakers | Channel | Method | $T_{60} \downarrow$ (ms) | DRR \downarrow (dB) | EDT \downarrow (ms) | CTE \downarrow (dB) |
|------------|--------------|-------------------|-----------------------------|--------------------------|--------------------------|--------------------------|
| Single | Left | MAD-V1 | 25.3 | 2.79 | 86.7 | 2.23 |
| Single | Left | MAD-V2 | 20.9 | 2.21 | 67.0 | 1.44 |
| Single | Left | MAD (ours) | 22.7 | 1.08 | 39.4 | 0.79 |
| Two | Left | MAD (ours) | 25.2 | 3.41 | 80.1 | 2.52 |
| Single | Right | MAD-V1 | 23.8 | 2.84 | 84.7 | 2.09 |
| Single | Right | MAD-V2 | 21.4 | 2.35 | 64.9 | 1.33 |
| Single | Right | MAD (ours) | 23.0 | 1.05 | 35.0 | 0.77 |
| Two | Right | MAD (ours) | 25.6 | 3.30 | 83.3 | 2.09 |

dataset into 33975 training, 750 validation and 752 test sets.

Baselines: Opus is the widely used audio codec in Zoom, Microsoft Team, Google Meet and YouTube and was standardized by the IETF in 2012. We use Opus as our traditional audio codec baseline. We also compare our approach using the state-of-the-art NAC for two-channel audio (Encodec) [5]. HiFi-Codec [6] and AUDIODEC [7] support only single-channel speech compression. Therefore, we separately compressed the left and right channels using HiFi-Codec and AUDIODEC. The pre-trained AUDIODEC in their official GitHub is trained only on clean speech. For a fair comparison, we trained AUDIODEC using our dataset. AUDIODEC is an improvised version of SoundStream [4] for speech coding. More details on our baseline are shown in Table 1.

Ablation: We evaluated three variations of our architecture to choose the best model for single speaker case. We evaluate the benefit of the HiFi-GAN vocoder by continuously training our network for 700k iterations with our simple speech decoder described in § 3.2 (MAD-V1). In AUDIODEC, only mel spectral loss is used as a metric loss. Therefore, we train the network without Eq. 4 to evaluate the benefits of spectrogram loss (Eq. 4) (MAD-V2). MAD is trained on our proposed approach in § 3. Due to computation complexity, we don’t use the HiFi-GAN vocoder for our two-speaker model.

Evaluation Metrics: We evaluate our model by measuring the clean speech estimation quality using the widely used speech enhancement metric STOI [25] and BIR estimation quality using a set of BIR acoustic parameters. Reverberation time (T_{60}), direct-to-reverberant ratio (DRR), early-decay-time (EDT), and early-to-late index (CTE) are commonly used acoustic parameters to measure IRs [26, 27]. We calculate the mean absolute difference of the BIR acoustic parameters between the estimated and the ground truth BIRs.

We also measure the ability of our model to preserve interaural time difference (ITD) and interaural level difference

(ILD) in reconstructed binaural speech. As proposed in previous work [28], we use generalized cross-correlation phase transform (GCC-PHAT) algorithm [29] to calculate the ITD error (Eq.10) between the left and right channels of ground truth speech (B^L, B^R) and reconstructed speech (\hat{B}^L, \hat{B}^R).

$$\mathbf{E}_{ITD} = \mathbb{E}[|ITD(B^L, B^R) - ITD(\hat{B}^L, \hat{B}^R)|]. \quad (10)$$

We define the ILD error for left channel (\mathbf{E}_{ILD_L}) and right channel (\mathbf{E}_{ILD_R}) as follows:

$$\mathbf{E}_{ILD_L} = \mathbb{E}[|20 \log_{10} \frac{\|\hat{B}^L\|_2}{\|B^L\|_2}|]. \quad (11)$$

$$\mathbf{E}_{ILD_R} = \mathbb{E}[|20 \log_{10} \frac{\|\hat{B}^R\|_2}{\|B^R\|_2}|]. \quad (12)$$

Results: Table 2 presents the ITD and ILD errors of the reconstructed binaural speech from different baselines and our approach. We can see that our approach gives the lowest ITD error for both single-speaker and two-speaker cases. Also, our approach outperforms ILD errors ($\mathbf{E}_{ILD_L}, \mathbf{E}_{ILD_R}$) when compared to every baseline except for Encodec-48. Encodec-48 needs four times more bandwidth, the compression rate is around 50 times less than our approach, and only suitable for non-streamable usage. For a fair comparison, we compare our model with Encodec-12, and we observe that our approach outperforms by 18% and 3% for single-speaker and two-speaker cases, respectively. We also compare three different variations of our single-speaker model and observe that replacing a simple speech decoder with a HiFi-GAN vocoder improves ITD error by 29%, and adding spectrogram loss improves the clean speech estimation quality (STOI) by 15%.

Table 3 shows the BIR estimation error of our approach. We observe that improving the binaural speech estimation quality by using HiFi-GAN vocoder and spectrogram loss indirectly contributed to improved BIR estimation and reduced the overall error of T_{60} , DRR, EDT, and CTE by 6.9%, 62.1%, 56.6% and 64% respectively in the single-speaker scenario. We can see that the performance of our two-speaker model is comparable to our single-speaker model MAD-V1.

5. CONCLUSION AND FUTURE WORK

We introduced M3-AUDIODEC, an innovative multi-channel neural audio codec designed for both single-speaker and multi-speaker multi-spatial overlapped speech. Our approach outperforms traditional and neural audio codecs with similar bandwidth in preserving binaural acoustic effects by up to 52%. We propose a novel approach to compress the speech content and spatial details separately and show that our approach can significantly reduce the bandwidth of compressing binaural speech by 48% when compared to compressing each channel using AUDIODEC. Given the intricacy of this domain and the need to experience output speech via headphones, our evaluations centered on binaural two-speaker overlapped speech. Future endeavors will expand to encompass compression and decoding of overlapped speech involving varied speaker counts and spatial configurations.

6. REFERENCES

- [1] Jan Skoglund and Jean-Marc Valin, “Improving opus low bit rate quality with neural speech synthesis,” in *INTERSPEECH*. 2020, pp. 2847–2851, ISCA.
- [2] Janusz Klejsa, Per Hedelin, Cong Zhou, Roy Fejgin, and Lars F. Villemoes, “High-quality speech coding with sample RNN,” in *ICASSP*. 2019, pp. 7155–7159, IEEE.
- [3] Roy Fejgin, Janusz Klejsa, Lars F. Villemoes, and Cong Zhou, “Source coding of audio signals with a generative model,” in *ICASSP*. 2020, pp. 341–345, IEEE.
- [4] Neil Zeghidour, Alejandro Luebs, Ahmed Omran, Jan Skoglund, and Marco Tagliasacchi, “Soundstream: An end-to-end neural audio codec,” *IEEE ACM Trans. Audio Speech Lang. Process.*, vol. 30, pp. 495–507, 2022.
- [5] Alexandre Défossez, Jade Copet, Gabriel Synnaeve, and Yossi Adi, “High fidelity neural audio compression,” *CoRR*, vol. abs/2210.13438, 2022.
- [6] Dongchao Yang, Songxiang Liu, Rongjie Huang, Jinchuan Tian, Chao Weng, and Yuexian Zou, “Hifi-codec: Group-residual vector quantization for high fidelity audio codec,” *CoRR*, vol. abs/2305.02765, 2023.
- [7] Yi-Chiao Wu, Israel D. Gebru, Dejan Marković, and Alexander Richard, “Audiodec: An open-source streaming high-fidelity neural audio codec,” in *ICASSP 2023 - 2023 IEEE International Conference on Acoustics, Speech and Signal Processing (ICASSP)*, 2023, pp. 1–5.
- [8] Frederic L. Wightman and Doris J. Kistler, “The dominant role of low-frequency interaural time differences in sound localization,” *The Journal of the Acoustical Society of America*, vol. 91 3, pp. 1648–61, 1992.
- [9] Jean-Marc Valin, Koen Vos, and Timothy B. Terriberry, “Definition of the opus audio codec,” *RFC*, vol. 6716, pp. 1–326, 2012.
- [10] B. S. Atal and Suzanne L. Hanauer, “Speech analysis and synthesis by linear prediction of the speech wave,” *The Journal of the Acoustical Society of America*, vol. 50, no. 2B, pp. 637–655, 1971.
- [11] Alan McCree et al., “A 2.4 kbit/s MELP coder candidate for the new U.S. federal standard,” in *ICASSP*. 1996, pp. 200–203, IEEE Computer Society.
- [12] D. Griffin and Jae Lim, “A new model-based speech analysis/synthesis system,” in *ICASSP ’85. IEEE International Conference on Acoustics, Speech, and Signal Processing*, 1985, vol. 10, pp. 513–516.
- [13] Martin Dietz et al., “Overview of the evs codec architecture,” in *2015 IEEE International Conference on Acoustics, Speech and Signal Processing (ICASSP)*, 2015, pp. 5698–5702.
- [14] Karren Yang et al., “Audio-visual speech codecs: Rethinking audio-visual speech enhancement by re-synthesis,” in *2022 IEEE/CVF Conference on Computer Vision and Pattern Recognition (CVPR)*, 2022, pp. 8217–8227.
- [15] Anton Ratnarajah et al., “Fast-rir: Fast neural diffuse room impulse response generator,” in *ICASSP 2022 - 2022 IEEE International Conference on Acoustics, Speech and Signal Processing (ICASSP)*, 2022, pp. 571–575.
- [16] Anton Ratnarajah et al., “Mesh2ir: Neural acoustic impulse response generator for complex 3d scenes,” in *Proceedings of the 30th ACM International Conference on Multimedia*, New York, NY, USA, 2022, MM ’22, p. 924–933, Association for Computing Machinery.
- [17] Anton Ratnarajah et al., “Towards improved room impulse response estimation for speech recognition,” in *ICASSP 2023 - 2023 IEEE International Conference on Acoustics, Speech and Signal Processing (ICASSP)*, 2023, pp. 1–5.
- [18] Christian J. Steinmetz, Vamsi Krishna Ithapu, and Paul Calamia, “Filtered noise shaping for time domain room impulse response estimation from reverberant speech,” in *2021 IEEE Workshop on Applications of Signal Processing to Audio and Acoustics (WASPAA)*, 2021, pp. 221–225.
- [19] Yi Luo and Nima Mesgarani, “Conv-tasnet: Surpassing ideal time–frequency magnitude masking for speech separation,” *IEEE/ACM Transactions on Audio, Speech, and Language Processing*, vol. 27, no. 8, pp. 1256–1266, 2019.
- [20] Jungil Kong et al., “Hifi-gan: Generative adversarial networks for efficient and high fidelity speech synthesis,” in *Advances in Neural Information Processing Systems*, H. Larochelle, M. Ranzato, R. Hadsell, M.F. Balcan, and H. Lin, Eds. 2020, vol. 33, pp. 17022–17033, Curran Associates, Inc.
- [21] Aaron van den Oord, Oriol Vinyals, and koray kavukcuoglu, “Neural discrete representation learning,” in *Advances in Neural Information Processing Systems*, I. Guyon, U. Von Luxburg, S. Bengio, H. Wallach, R. Fergus, S. Vishwanathan, and R. Garnett, Eds. 2017, vol. 30, Curran Associates, Inc.
- [22] Cassia Valentini-Botinhao, “Noisy speech database for training speech enhancement algorithms and TTS models,” 2017.
- [23] Junichi Yamagishi et al., “CSTR VCTK Corpus: English Multi-speaker Corpus for CSTR Voice Cloning Toolkit (version 0.92),” 2019.
- [24] Zhenyu Tang et al., “Improving reverberant speech training using diffuse acoustic simulation,” in *ICASSP 2020 - 2020 IEEE International Conference on Acoustics, Speech and Signal Processing (ICASSP)*, 2020, pp. 6969–6973.
- [25] Cees H. Taal, Richard C. Hendriks, Richard Heusdens, and Jesper Jensen, “A short-time objective intelligibility measure for time-frequency weighted noisy speech,” in *2010 IEEE International Conference on Acoustics, Speech and Signal Processing*, 2010, pp. 4214–4217.
- [26] Anton Ratnarajah, Zhenyu Tang, and Dinesh Manocha, “IR-GAN: Room Impulse Response Generator for Far-Field Speech Recognition,” in *Proc. Interspeech 2021*, 2021, pp. 286–290.
- [27] Anton Ratnarajah, Zhenyu Tang, and Dinesh Manocha, “Ts-rir: Translated synthetic room impulse responses for speech augmentation,” in *2021 IEEE Automatic Speech Recognition and Understanding Workshop (ASRU)*, 2021, pp. 259–266.
- [28] Cong Han, Yi Luo, and Nima Mesgarani, “Real-time binaural speech separation with preserved spatial cues,” in *ICASSP 2020 - 2020 IEEE International Conference on Acoustics, Speech and Signal Processing (ICASSP)*, 2020, pp. 6404–6408.
- [29] C. Knapp and G. Carter, “The generalized correlation method for estimation of time delay,” *IEEE Transactions on Acoustics, Speech, and Signal Processing*, vol. 24, no. 4, pp. 320–327, 1976.